Supporting Information

Stable 1T-phase MoS_2 as an effective electron mediator promoting photocatalytic hydrogen production

Jian-Wen Shi,*[a,c] Yajun Zou,[a] Dandan Ma,[a] Zhaoyang Fan,[a] Linhao Cheng,[a] Diankun Sun,[a] Zeyan Wang,[c] Chunming Niu,[a] Lianzhou Wang*[b]

[a] *Center of Nanomaterials for Renewable Energy, State Key Laboratory of Electrical Insulation and Power Equipment, School of Electrical Engineering, Xi'an Jiaotong University, Xi'an 710049, China*

[b] *Nanomaterials Centre, School of Chemical Engineering and AIBN, The University of Queensland, St. Lucia, Brisbane, QLD, 4072, Australia*

[c] *State Key Laboratory of Crystal Materials, Shandong University, Jinan, 250100, China*

Corresponding author:

Jian-Wen Shi, E-mail: jianwen.shi@mail.xjtu.edu.cn

Lianzhou Wang, E-mail: l.wang@uq.edu.au

1. Tables

Table S1. Area value (kceV/sec) for deconvoluted peaks of CNMS samples.

Elements	CNMS-1	CNMS-2	CNMS-3	CNMS-4	CNMS-5
Mo^{6+} $3d_{3/2}$ (MoO_3)	262.1	210.8	285.4	421.5	405.6
Mo^{6+} $3d_{5/2}$ (MoO_3)	558.2	424.0	522.9	701.8	840.1
Mo^{4+} $3d_{5/2}$ (MoO_2)	76.7	73.9	95.6	113.0	157.5
Mo^{4+} $3d_{5/2}$ (MoS_2)	69.4 (6.8%)	89.9 (10.6%)	124.5 (11.3%)	176.2 (11.7%)	228.6 (13.0%)
S^{2-} 2s	44.1 (4.3%)	52.9 (6.2%)	71.1 (6.5%)	98.0 (6.5%)	129.3 (7.3%)
S $2p_{1/2}$	33.4	53.6	56.1	60.3	71.2
S $2p_{3/2}$	44.7	55.6	63.4	92.7	107.5

Table S2. Structural parameters of the samples.

Samples	S_{BET} ($m^2 \cdot g^{-1}$)	Pore size (nm)	V_{pore} ($cm^3 \cdot g^{-1}$)
g-C_3N_4	5.89	3.94	0.15
CNMO	32.35	3.94	0.39
CNMS-1	35.94	3.94	0.35
CNMS-2	36.57	3.85	0.48
CNMS-3	37.29	3.92	0.47
CNMS-4	39.97	3.50	0.40
CNMS-5	42.52	3.24	0.43

2. Figures

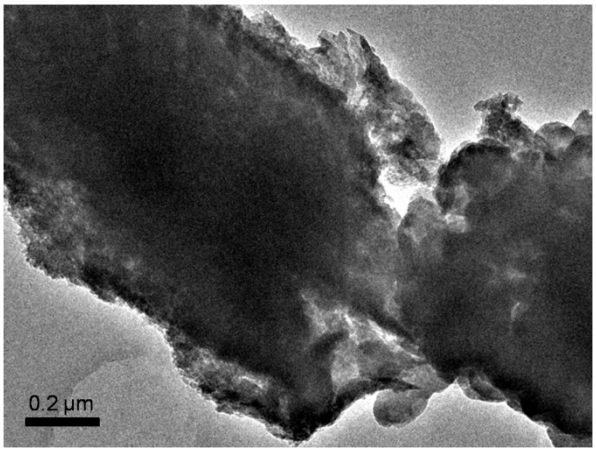

Fig. S1. TEM image of the pure g-C_3N_4.

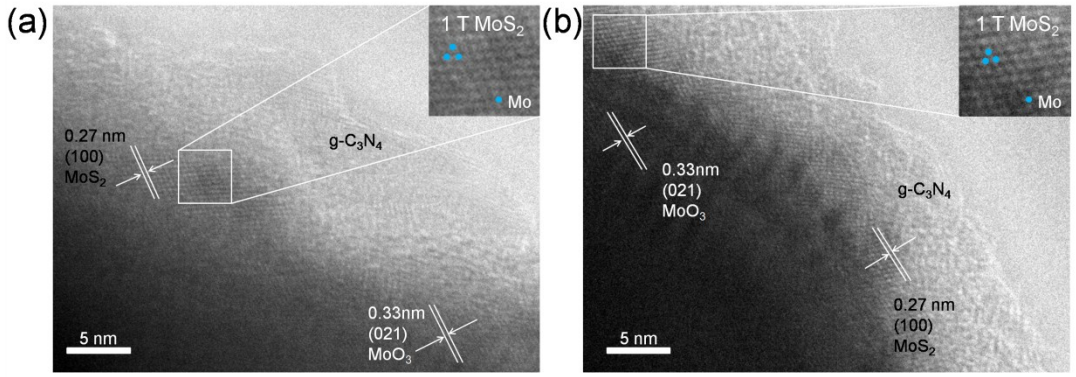

Fig. S2. TEM images of CNMS-3 (a) and CNMS-4 (b) (the insets shows the region enclosed by the white square of images in (a) and (b), respectively).

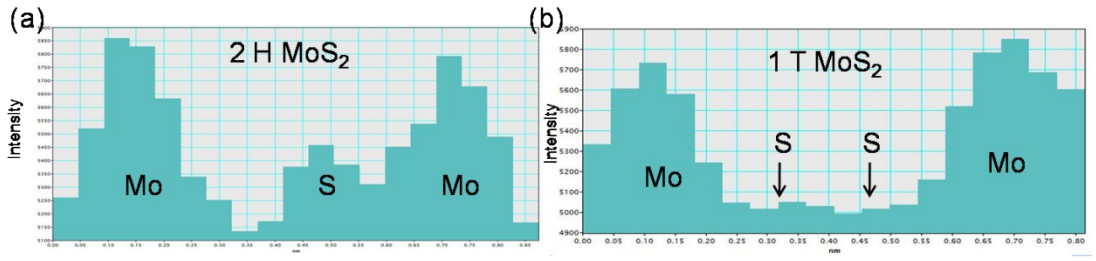

Fig. S3. (a-b) Intensity profiles along the green lines indicated in Fig. 1c and d, respectively.

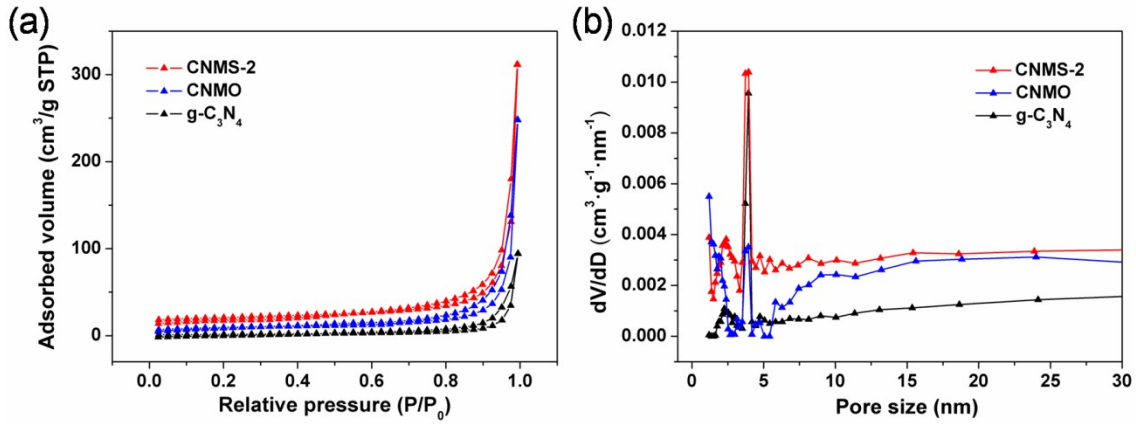

Fig. S4. N_2 adsorption–desorption isotherms (a) and pore size distribution curves (b) of g-C_3N_4, CNMO and CNMS-2 samples.

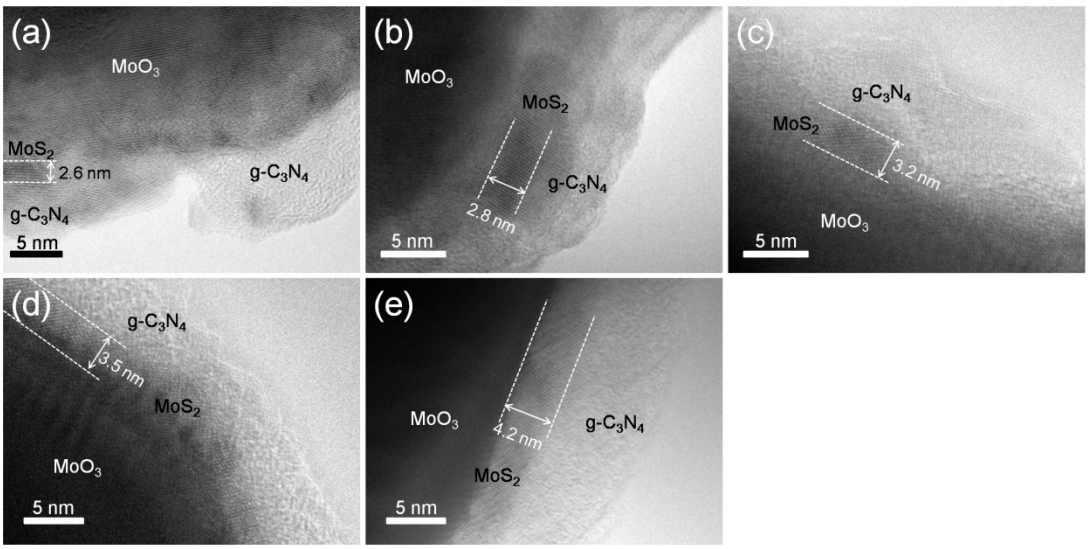

Fig. S5. The thickness of MoS_2 layers in CNMS-1 (a), CNMS-2 (b), CNMS-3 (c), CNMS-4 (d) and CNMS-5 (e).

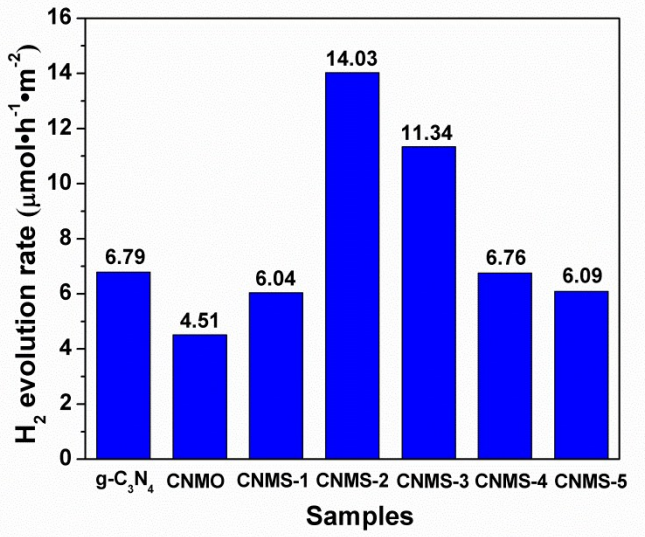

Fig. S6. H_2 production rates of the samples under visible-light irradiation (λ> 420 nm) normalized to the corresponding BET surface areas.

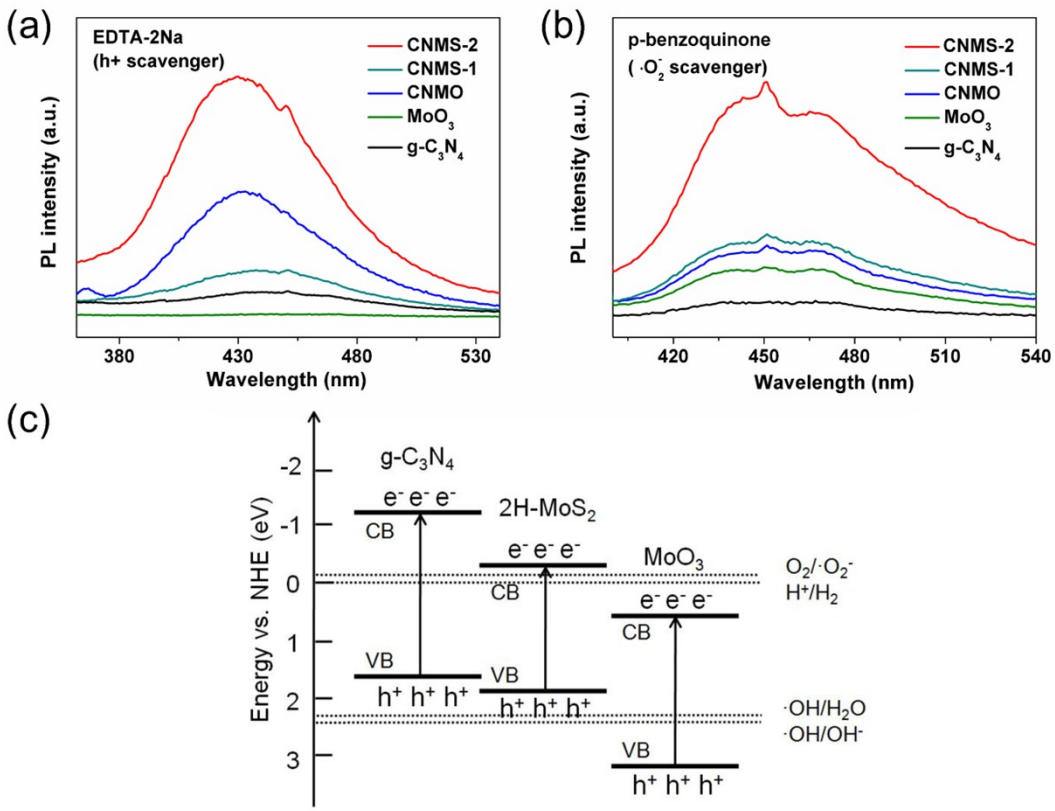

Fig. S7. The PL spectral intensities (excitation at 315 nm) observed for MoO_3, g-C_3N_4, CNMO, CNMS-1 and CNMS-2 under visible light irradiation (>420 nm) for 15 min in a 5×10^{-4} M basic solution of terephthalic acid with h^+ scavenger: EDTA-Na_2 (a) and with $\bullet O_2^-$ scavenger: p-benzoquinone (b), band positions of MoO_3, g-C_3N_4, and 2H-MoS_2 together with $O_2/\bullet O_2^-$, H^+/H_2,·OH/H_2O and ·OH/OH^- redox potentials (c).

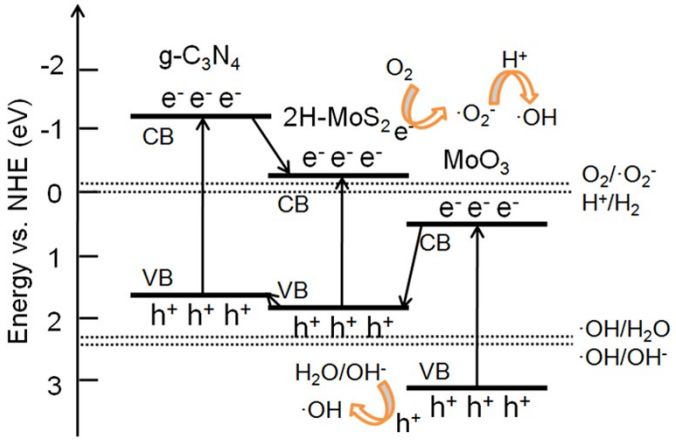

Fig. S8. Pathways of •OH produced from MoO_3/2H-MoS_2/g-C_3N_4.

Compared with CNMO, CNMS-1 exhibits a weaker PL peak intensity in the presence of EDTA-Na_2 as h^+ scavenger. This suggests that the •OH radicals are originated from the photoexcited electrons in the CB of the 2H-phase MoS_2, which can be explained by the fact that the electrons on the CB of the 2H-phase MoS_2 possess lower reduction ability than those on the CB of g-C_3N_4, and therefore, the PL emission peak intensity of CNMS-1 should be weaker than that of CNMO. Meanwhile, when p-benzoquinone was added as the $•O_2^-$ scavenger, a stronger PL peak intensity was observed in CNMS-1 compared with CNMO, suggesting that the holes generated •OH radicals must be in the VB of MoO_3. Thus, it can be concluded that the photogenerated charge carriers transferred via the traditional heterojunction mechanism between g-C_3N_4 and the 2H-phase MoS_2 and migrated through the direct Z-scheme mechanism between the 2H-phase MoS_2 and MoO_3 (**Fig. S8**).

3. Solar-to-hydrogen conversion efficiency (STH) calculations

The solar-to-hydrogen energy conversion efficiency (STH) was evaluated by using a 300 W Xenon arc lamp (PLS-SXE300) with a 420 nm cutoff filter as light source (25.8 mW/cm^2) and CNMS-2 sample as the catalyst (10 mg catalyst in 20 mL deionized water). The light intensity was obtained with an optical power meter (CEL-NP2000, CEAULIGHT, Beijing). After 4 h of illumination, the total incident power over the 28.3 cm^2 irradiation area (3 cm radius) was:

$P_{Solar} = 25.8 \times 28.3 \times 10^{-3} = 0.73$ W

The total input energy in 4 hours was:

$E_{Solar} = 0.73 \times 4 \times 3600 = 1.051 \times 10^4$ J

During the photocatalytic reaction, 20.52 μmol H_2 was detected by gas chromatography (GC), which indicated that the energy generated by water splitting was:

$E_{Hydrogen} = 20.52 \times 10^{-6} \times 6.02 \times 10^{23} \times 2.46 \times 1.609 \times 10^{-19} = 4.89$ J; 2.46 eV is the free energy of water splitting.

The STH was determined to be:

$STH = E_{Hydrogen}/E_{Solar} = 4.89/(1.051 \times 10^4) = 0.047\%$